Available online at www.sciencedirect.com
SCIENCE DIRECT®
Cement & Concrete Composites 27 (2005) 65–76
Cement & Concrete Composites
www.elsevier.com/locate/cemconcomp

Sulfate attack and role of silica fume in resisting strength loss

S.T. Lee [a,*], H.Y. Moon [b], R.N. Swamy [c]

[a] Department of Civil Engineering, University of Toronto, 35 St. George St, Toronto, ON, Canada M5S 1A4
[b] Department of Civil Engineering, Hanyang University, 17 Haengdang-dong, Seongdong-gu, Seoul 133-791, South Korea
[c] Department of Mechanical Engineering and Centre for Cement and Concrete, University of Sheffield, Mappin St, Sheffield S1 3JD, UK

Received 17 February 2003; accepted 19 November 2003

Abstract

This paper presents a detailed experimental study on the sulfate attack of Portland cement mortars, and the effectiveness of silica fume in controlling the damage arising from such attack. The test solutions used to supply the sulfate ions and cations were 5% sodium sulfate solution and 5% magnesium sulfate solution. Tap water was used as the reference solution. The main variables investigated in the study were the water/cementitious materials ratio, and the level of cement replacement. Compressive strength measured on 50 mm cubes was used to assess the changes in the mechanical properties of mortar specimens exposed to sulfate attack for 510 days. X-ray diffraction and differential scanning calorimetry were used to evaluate the microstructural nature of the sulfate attack. The test results showed that the presence of silica fume had a beneficial effect on the strength loss due to sodium sulfate attack. The best resistance to sodium sulfate attack was obtained with a SF replacement of 5–10%, but even then, a strength loss of 15–20% can be expected. On the other hand, mortars with silica fume were severely damaged in the magnesium sulfate environment. Further, the compressive strength loss actually increased with increasing SF content. The test results thus showed clearly that the use of SF in concrete exposed to magnesium sulfate solution is not recommended. The test results also showed that the w/cm ratio is the most critical parameter influencing the resistance of concrete to sulfate attack. All the tests reported in the study were carried out at 20 ± 1 °C.

Keywords: Sulfate attack; Strength loss; Silica fume; Sodium and magnesium sulfate solutions; Compressive strength; X-ray diffraction; Microstructure

1. Introduction

It has been recognized for a long time that sulfate ions in soils, particularly below ground, can cause severe damage to concrete structures. Until now, however, it has been difficult to define the precise nature of the mechanism of sulfate attack because of its complex behaviour. There have been numerous field studies on the distress caused to concrete structures generated by sulfate attack [1–5]. Many research studies have also been carried out to unravel this complex phenomenon through immersion tests in the laboratory as well as in the field [6–13]. All these investigations emphasize that in order to understand the deterioration of concrete due to sulfate attack, it is necessary to consider the type of the accompanying cation as well as the degree of concentration of the sulfate solution [9].

Sulfate attack has often been discussed in terms of the reaction between the hydrates in cement pastes and dissolved compounds, such as sodium sulfate or magnesium sulfate, in the attacking solution [14]. A magnesium sulfate solution may cause the deterioration of concrete due to the formation of Mg-containing hydrates (e.g. M–S–H gel), as well as gypsum and thaumasite. Sodium sulfate solution, on the other hand, may be responsible for the deterioration of concrete by the reaction of SO_4^{2-} ions [9,15–18].

Cohen and Bentur [15], Akoz et al. [11], and Turker et al. [19] have reported on the sulfate resistance imparted by silica fume, which is generally incorporated in concrete to improve its engineering properties and durability. The excellent resistance of silica fume to sodium sulfate solution is demonstrated from the tests reported by Mangat and El-Khatib [20] and Wee et al. [21]. This excellent resistance is due to the filler action of

* Corresponding author. Tel.: +1-416-946-5496; fax: +1-416-978-7046.
E-mail address: stlee70@lycos.co.kr (S.T. Lee).

0958-9465/$ - see front matter © 2004 Elsevier Ltd. All rights reserved.
doi:10.1016/j.cemconcomp.2003.11.003

silica fume because of its fine particle size, and the pore refinement process occurring due to the conversion of portlandite into secondary C–S–H gel, through strong pozzolanic reaction.

In this study, the effect of silica fume on attack by sodium sulfate and magnesium sulfate was investigated. The experimental study was developed to obtain conclusive data on any positive or negative effects of silica fume in sodium and magnesium sulfate environments.

2. Experimental details

In the tests reported in this paper, compressive strength tests and X-ray diffraction (XRD) studies were carried out on mortar samples. The differential scanning calorimetry (DSC) tests were carried out on paste samples. Ordinary Portland cement (OPC), produced by Ssang-yong Cement Ltd, Korea, was used throughout. Silica fume (SF) with a specific surface area of 20,470 m^2/kg was used at replacement levels of 5%, 10% and 15% by mass of cement. The chemical composition of OPC and SF used in this investigation is shown in Table 1. The mineralogical composition of OPC by Bogue calculation is also listed in Table 1, and indicates a normal Portland cement.

The water/cementitious materials ratios (w/cm) of the mortar mixture proportions tested in the present study were 0.35, 0.45 and 0.55. In order to obtain adequate workability, a superplasticizer (SP), selected from several available products after an evaluation of their workability characteristics, was used. The polycarbonic acid-based chemical admixture was incorporated in the mortar mixture proportions with w/cm of 0.35 and 0.45.

Table 1
Chemical composition and physical properties of OPC and SF

		OPC	SF
SiO_2 (%)		20.2	91.2
Al_2O_3 (%)		5.8	1.3
Fe_2O_3 (%)		3.0	0.8
CaO (%)		63.3	0.7
MgO (%)		3.4	0.3
SO_3 (%)		2.1	–
Loss on ignition		2.1	2.3
K_2O (%)		0.3	–
Na_2O (%)		0.2	–
Setting time (min.)	Initial set	250	–
	Final set	400	–
Specific gravity		3.13	2.20
Specific surface area (m^2/kg)		312	20,470[a]
Mineralogical composition determined by Bogue calculation (%)	C_3S	54.9	–
	C_2S	16.6	–
	C_3A	10.3	–
	C_4AF	9.1	–

[a] Value measured by the nitrogen adsorption technique.

The superplasticizer was added to the mixing water at a level of 0.5% by mass of total cementitious material; it was well stirred until completely dissolved before addition to the mortar mixtures. River sand, with a maximum size of 5 mm, was used as the fine aggregate in the mixture. The specific gravity, water absorption and fineness modulus of the fine aggregate were 2.60%, 0.80% and 2.80%, respectively. The sand:cement ratio used was 2:1 by mass.

The details of the mortar mixtures used in the tests are listed in Table 2. The mixing of the mortar was carried out using the appropriate amounts of cementitious materials, sand and water with the added SP. The sequence of mixing was as follows: mixing for half a minute, rest for 1.5 min, followed by further mixing for 1 min.

The paste samples used for the DSC tests were made using 100 g of total cementitious material and 45 g of water with no superplasticizer. They were cast in plastic cylinders of 12 mm diameter and demoulded after 1 day. To avoid segregation, after mixing, the samples in their containers were rotated for 8 h. After demoulding, the paste samples were cured in water for an additional 6 days. The paste samples were then coated with an epoxy on all surfaces except the upper part. Ten millimeter portions from the uncoated side of pastes were then selected for the DSC analysis.

Compressive strength measurements were made on 50 mm cube mortar specimens. All specimens, with or without SF, were demoulded after 1 day of casting, and cured in water at room temperature for an additional 6 days. Some of them were then moved to test solutions and kept continuously immersed for predetermined periods.

The 5% sodium sulfate and the 5% magnesium sulfate solutions used for the immersion tests were renewed every 4 weeks to minimize the increase in pH due to the leaching of OH^- ions from the mortar and paste specimens. Test solutions were kept at 20 ± 1 °C during the test period. For comparison, tap water, kept at a similar temperature, was used as a reference solution for control samples.

Table 2
Details of mortar mixtures

Mixture number	Symbol	Cementitious materials	w/cm
1	OPC-35	100% OPC	0.35
2	OPC-45	100% OPC	0.45
3	OPC-55	100% OPC	0.55
4	SF5-45	95% OPC + 5% SF	0.45
5	SF10-35	90% OPC + 10% SF	0.35
6	SF10-45	90% OPC + 10% SF	0.45
7	SF10-55	90% OPC + 10% SF	0.55
8	SF15-45	85% OPC + 15% SF	0.45

The deterioration of the mortar cube specimens was investigated by determining the compressive strength loss (CSL), which was calculated as follows.

$$\text{Compressive strength loss } (\%) = [(A - B)/A] \times 100$$

where, A is the average compressive strength of mortar specimens cured in tap water (MPa) and B is the average compressive strength of mortar specimens immersed in test solutions (MPa) for the same period. Compressive strength tests were performed on each mixture prior to immersion, and at 28, 91, 180, 270, 360 and 510 days of immersion. At each test age, the compressive strengths of five mortar specimens stored in tap water and test solutions were determined, and then their values were averaged.

After testing for compressive strength of mortar specimens immersed in test solutions for 510 days, the surface and centre parts of the test samples were selected for XRD analysis. They were ground by hand, and the XRD test was conducted using the RINT D/max 2500 (Rigaku) X-ray diffractometer. For the XRD tests, CuKα radiation with a wavelength of 1.54 Å at a voltage of 30 kV, scanning speed of 3°/min and current of 30 mA were used.

The DSC analysis using the DSC 2010 Differential Scanning Calorimeter (TA Instruments) was conducted to evaluate the products of hydration and chemical reaction. The amount of paste sample powder used was approximately 10 mg. The powder was heated from ambient temperature to 560 °C at a rate of 10 °C/min in a nitrogen atmosphere.

3. Test results

3.1. Visual examination

A thorough visual examination was carried out every month to evaluate the visible signs of softening, cracking and spalling in the mortar specimens exposed to sulfate attack. Figs. 1–4 show typical examples of damage of mortar specimens subjected to sulfate attack after 510 days of immersion in both sulfate solutions. Table 3 summarizes the visually observed progression of material damage of the control mortar specimens and those containing 10% SF, all with a w/cm ratio of 0.45 and exposed to both sulfate solutions.

It was observed that initial deterioration invariably started from the corners of the mortar samples. For OPC-45 mortars immersed in sodium sulfate solution for 510 days, the loss of mortar mass was approximately 11%, and the wide cracks due to the expansive pressure on the cement matrix were significant, as seen in Fig. 1. Signs of visual deterioration of the OPC-45 mortar were first observed at 56 days with some visible cracks near the corners. On the other hand, SF5-45, SF10-45 and

Fig. 1. OPC-45 mortar cubes immersed in 5% sodium sulfate solution for 510 days.

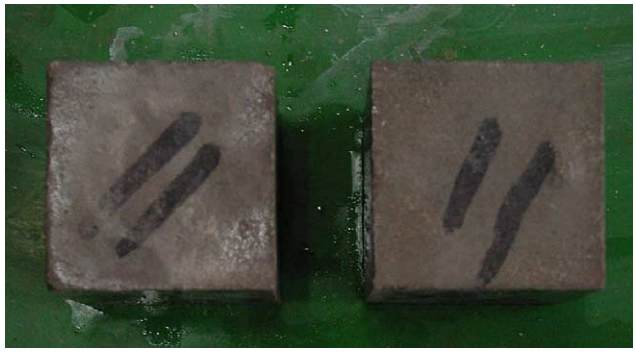

Fig. 2. SF10-45 mortar cubes immersed in 5% sodium sulfate solution for 510 days.

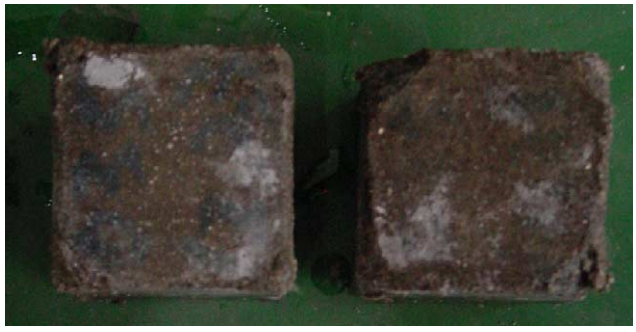

Fig. 3. OPC-45 mortar cubes immersed in 5% magnesium sulfate solution for 510 days.

SF15-45 mortars showed no signs of deterioration at 150 days, even at the corners. After 510 days of immersion in sodium sulfate solution, the visual examination of SF10-45 mortars showed little visible deterioration with no detectable weight loss, as shown in Fig. 2, while OPC-45 mortars displayed significant expansion, spalling and cracking as well as softening on all the faces.

In magnesium sulfate solution, some parts of the surfaces of OPC-45 mortars peeled off after 180 days of

Fig. 4. SF10-45 mortar cubes immersed in 5% magnesium sulfate solution for 510 days.

immersion, due to loss of cohesiveness between the surface layer and the inner cement matrix. After 510 days of exposure, the corners of OPC-45 mortars had spalled off, and a layer of white material was found deposited on the faces of the mortars, as shown in Fig. 3. Furthermore, inside the cracks of the mortars, needle-shaped crystals (probably gypsum formation) were present. Fig. 4 shows the visual appearance of the deteriorated SF10-45 mortars immersed in magnesium sulfate solution for 510 days. It can be seen that the SF mortars show exposed aggregates and somewhat greater severity of deterioration compared to that of OPC-45 mortars, even though both mortars were exposed to magnesium sulfate attack for the same immersion period.

3.2. Compressive strength loss, CSL

As reported earlier, the compressive strengths of all the test specimens were determined from 50 mm cube specimens. Table 4 summarizes these results for a w/cm ratio of 0.45 at the ages of 28, 180, 360 and 510 days of immersion in tap water and sulfate solutions as well as the strength prior to exposure to sulfate solutions. These strength results are discussed below in terms of strength loss defined earlier in order to highlight the damage caused to mortar by exposure to sulfate attack.

The CSL of mortars without and with SF immersed in 5% sodium sulfate solution is shown in Figs. 5–7. The relative strength loss in the early stages of curing/expo-

Table 4
Compressive strength of 50 mm cube mortar specimens with w/cm of 0.45 immersed in tap water and sulfate solutions (MPa)

Immersion age (days)	Symbol	Tap water	5% sodium sulfate solution	5% magnesium sulfate solution
Prior to immersion	OPC	39.7	39.7	39.7
	SF5	37.9	37.9	37.9
	SF10	37.2	37.2	37.2
	SF15	45.1	45.1	45.1
28	OPC	51.7	54.7	54.6
	SF5	61.4	68.1	53.0
	SF10	62.8	66.1	49.7
	SF15	61.8	67.8	48.1
180	OPC	57.8	49.7	48.5
	SF5	68.8	66.3	49.5
	SF10	70.5	70.1	47.9
	SF15	69.7	68.8	43.1
360	OPC	58.3	32.1	42.0
	SF5	73.5	62.5	38.3
	SF10	74.4	57.3	34.9
	SF15	81.5	68.4	26.9
510	OPC	59.1	21.4	31.1
	SF5	75.4	61.6	32.8
	SF10	74.6	58.1	29.4
	SF15	83.7	69.0	29.1

Table 3
Summary of visual damage of mortar specimens exposed to sulfate solutions

Immersion age (days)	5% sodium sulfate solution		5% magnesium sulfate solution	
	OPC-45	SF10-45	OPC-45	SF10-45
91	Some visible cracks	No visible deterioration	White materials deposition	White materials deposition
			No visible deterioration	No visible deterioration
180	Expansion and cracking	No visible deterioration	Some spalling at edge	Surface peeling off and mass loss
	Beginning to spall			Partial disintegration
360	Mass loss (about 5%)	No cracks but some signs of deterioration at the corners	Mass loss (about 3%)	Mass loss (about 3%)
	Extensive spalling		Partial disintegration and cracking	Extensive softening and spalling
	Wider cracks		Surface peeling off	
510	Considerable mass loss (10% or more)	Some visible cracks	Cross-section reducing	Visible gypsum crystals inside cracks
	Severe surface softening	Negligible mass loss	Extensive softening and spalling	Considerable disintegration Cross-section reducing
	Significant expansion			
	Entire disintegration			

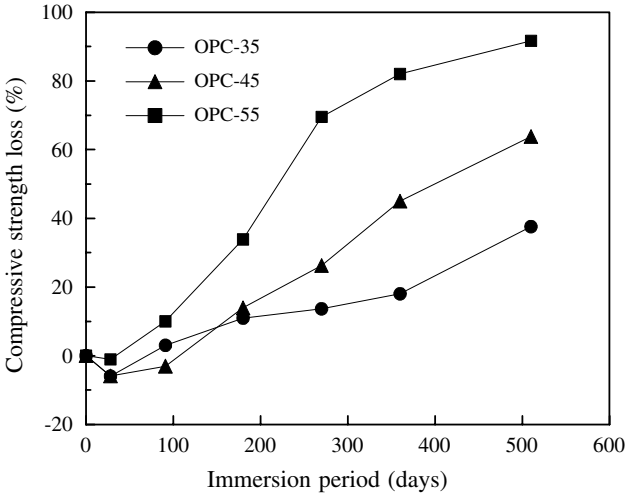

Fig. 5. Compressive strength loss of OPC mortars subjected to sulfate attack in 5% sodium sulfate solution.

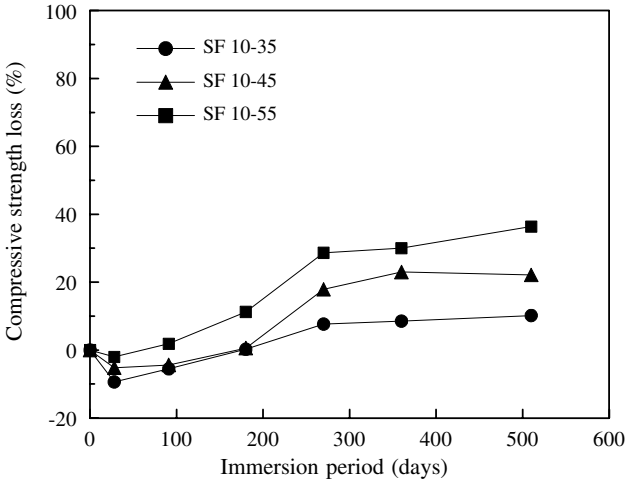

Fig. 6. Compressive strength loss of SF mortars subjected to sulfate attack in 5% sodium sulfate solution.

sure indicate that the strength of the specimens exposed to sodium sulfate solution is greater than those cured in water for the same period. This has been previously reported [22], and the negative values of CSL are attributed to the filling up of the pore space by the expansive products, densifying the mortar matrix in the early period of immersion, and prior to them being subjected to high tensile strain.

Figs. 5 and 6 also confirm that the w/cm ratio is a key factor in the strength loss of mortar samples exposed to sulfate attack. The strength loss increased as the w/cm ratio increased; and the total strength loss as well as that between different w/cm ratio levels was greater in mortar specimens without SF compared to those with SF. For example, after 510 days of immersion in sodium sulfate solution, the CSL of OPC-35, OPC-45 and OPC-55

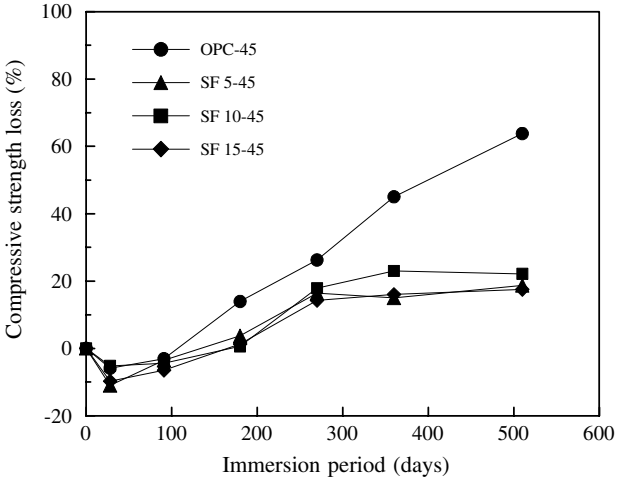

Fig. 7. Compressive strength loss of mortars subjected to sulfate attack in 5% sodium sulfate solution (w/cm = 0.45).

mortars was about 38%, 64% and 92% respectively, compared to CSL of 10%, 22% and 36% respectively for the SF10-35, SF10-45 and SF10-55 samples. In summary, it is clear that at a given w/cm ratio, SF10 mortars exhibited a much better resistance to sodium sulfate attack than OPC mortars.

Fig. 7 shows the CSL values for mortars with different SF contents, but having the same w/cm ratio of 0.45. These results emphasize that the incorporation of SF leads to reduced CSL compared with those having only OPC. However, the amount of strength loss for the three levels of SF replacement was not significantly different, and after about 270 days of exposure to sodium sulfate attack, the CSL remained relatively constant at about 15–20% for SF contents of 5–15%. The overall message from the data shown in Figs. 5–7 is that the best resistance to sodium sulfate attack is obtained with low w/cm ratios and when the SF replacement is of the order of 5–10%. Even then, with continued attack, a strength loss of 15–20% can be expected.

The general trend of strength loss of OPC mortars exposed to 5% magnesium sulfate is shown in Fig. 8, which is similar to that in sodium sulfate solution, with strength increase at early ages for reasons described earlier. However, the overall CSL in magnesium sulfate solution is much less pronounced than that in sodium sulfate shown in Fig. 5. The results of CSL of SF mortars with w/cm ratio of 0.35, 0.45 and 0.55 and subjected to magnesium sulfate attack for 510 days are shown in Fig. 9. These data also indicate that the CSL values of SF mortars in magnesium sulfate solution follow a similar trend to those of SF mortars in sodium sulfate solution. However, the extent of CSL is much higher in magnesium sulfate solution at all immersion ages, and at all w/cm ratio levels when compared to strength loss in sodium sulfate solution. For example, at

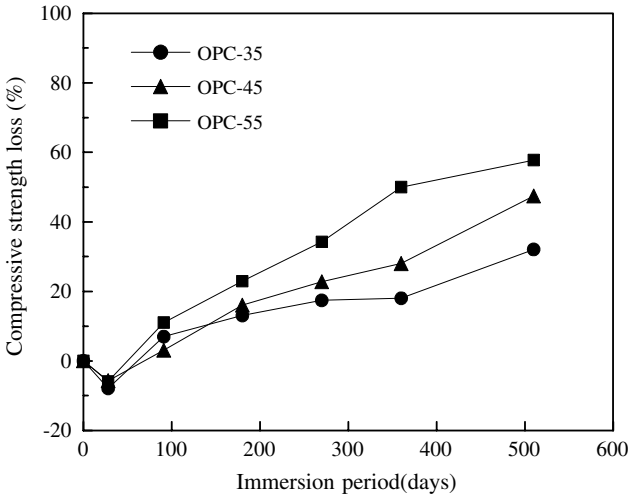

Fig. 8. Compressive strength loss of OPC mortars subjected to sulfate attack in 5% magnesium sulfate solution.

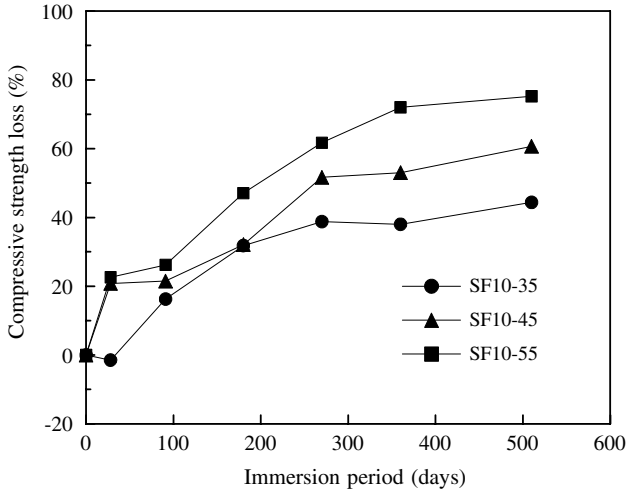

Fig. 9. Compressive strength loss of SF mortars subjected to sulfate attack in 5% magnesium sulfate solution.

510 days of immersion, the CSL of SF mortars in magnesium sulfate solution varied from about 44% to 75%, whereas the strength loss was only from about 10% to 36% in sodium sulfate solution. It is evident from these data that the use of SF in concrete exposed to magnesium sulfate solution might result in severe deterioration in terms of strength loss compared with that in sodium sulfate solution. Indeed, the data in Fig. 10 confirm this, and emphasize further that the compressive strength loss actually increases with increasing SF content. This is very contrary to what happens when SF is used in concrete mixtures exposed to sodium sulfate solution.

From these immersion test results, it can be clearly seen that w/cm ratio is the most critical parameter influencing the sulfate resistance of mortar. Further,

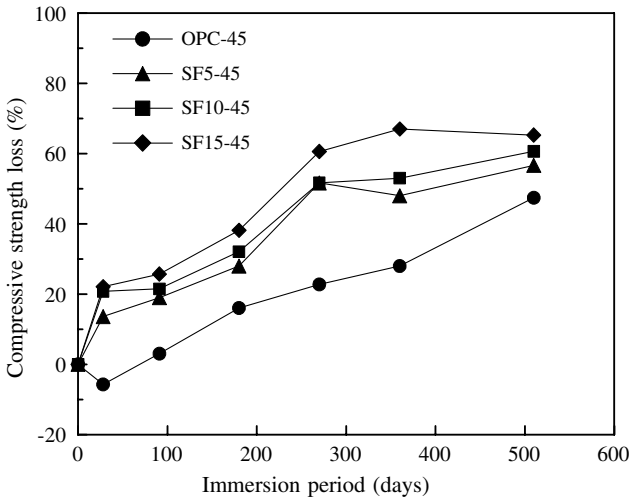

Fig. 10. Compressive strength loss of mortars subjected to sulfate attack in 5% magnesium sulfate solution (w/cm = 0.45).

much more importantly, the use of SF as a cement replacement material can aggravate strength loss when the source of sulfate ions is magnesium.

4. Microstructural analysis

4.1. X-ray diffraction

XRD analyses of OPC-45 and SF10-45 mortars placed in 5% sodium sulfate and 5% magnesium sulfate solution for 510 days are presented here. The XRD analysis was conducted on both the deteriorated i.e. the outer surface, and the sound i.e. inner parts of cube mortar samples tested for compressive strength.

Diffractograms shown in Fig. 11 indicate that the difference between the inner and the outer surface parts of OPC-45 mortar exposed to sodium sulfate solution is remarkable. Especially in the surface part of OPC-45 mortar, the peaks of thaumasite were detected at 9.2° and 15.0° 2θ in addition to gypsum peaks at 11.7°, 20.7° and 29.2° 2θ. On the other hand, as shown in Fig. 12, the XRD trace of powders from SF mortar sample (surface part) stored in the same solution showed no thaumasite peaks even after 510 days of immersion in 5% sodium sulfate solution, and only a somewhat weak gypsum peak at 29.2 2θ was observed. The XRD traces on the deteriorated part of both OPC and SF mortar revealed the absence of portlandite due to sodium sulfate attack.

In the deteriorated part drawn from OPC-45 mortar sample after 510 days of exposure to 5% magnesium sulfate solution, the main peaks for gypsum at 11.7° and 29.2° 2θ were very strong, as shown in Fig. 13, while brucite peaks appeared weakly only at 38.0° 2θ, because much of the surface layer of the mortars had peeled

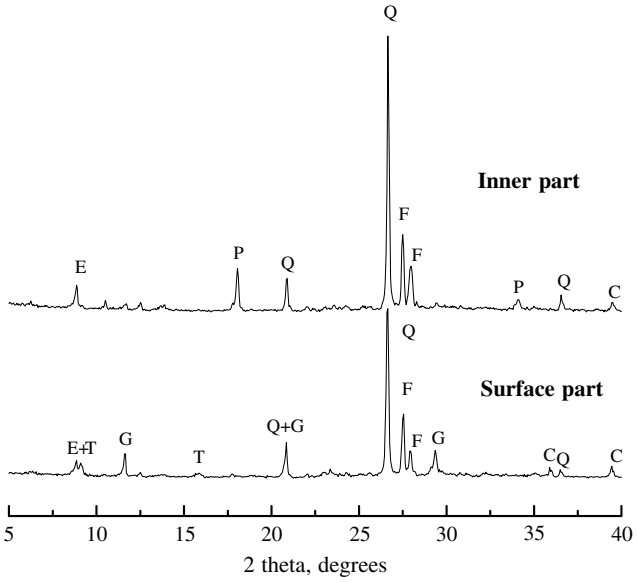

Fig. 11. XRD of OPC-45 mortar placed in 5% sodium sulfate solution for 510 days. (Note: E = ettringite, P = portlandite, Q = quartz, F = feldspar, C = calcite, T = thaumasite, G = gypsum).

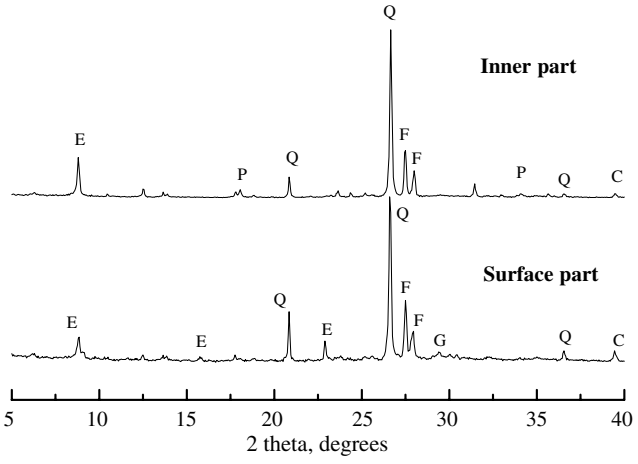

Fig. 12. XRD of SF10-45 mortar placed in 5% sodium sulfate solution for 510 days. (Note: E = ettringite, P = portlandite, Q = quartz, F = feldspar, C = calcite, G = gypsum).

off. As expected, the peaks for ettringite, calcite, quartz and feldspar were observed in both the outer and inner parts.

Despite the severe deterioration of SF10-45 mortar surface due to magnesium sulfate attack, the peaks for ettringite were not detected even at its main peak of 9.1° 2θ (Fig. 14). Another important observation of XRD analysis on the surface part of SF10-45 mortar samples stored in magnesium sulfate solution was the presence of strong intensity peaks for gypsum compared with those in the sodium sulfate solution. On the other hand, there was no proof, from XRD analysis, for the presence of M–S–H, which causes the strength loss in mortars.

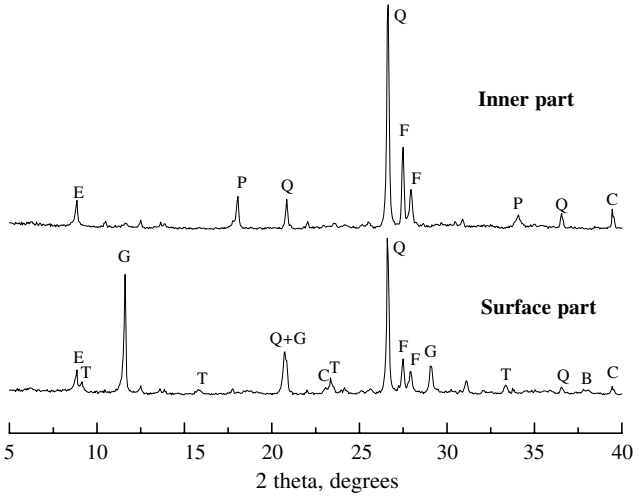

Fig. 13. XRD of OPC-45 mortar placed in 5% magnesium sulfate solution for 510 days. (Note: E = ettringite, P = portlandite, Q = quartz, F = feldspar, C = calcite, T = thaumasite, G = gypsum, B = brucite).

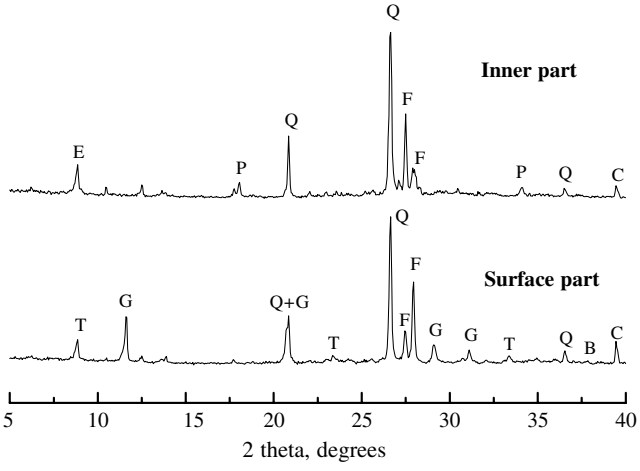

Fig. 14. XRD of SF10-45 mortar placed in 5% magnesium sulfate solution for 510 days. (Note: E = ettringite, P = portlandite, Q = quartz, F = feldspar, C = calcite, T = thaumasite, G = gypsum, B = brucite).

4.2. Differential scanning calorimetry

The results of the DSC tests carried out to assess the thermal characteristics of products produced in pastes stored in 5% sodium sulfate and 5% magnesium sulfate solution for 270 days are shown in Figs. 15–18. It is recalled that these samples were made with a w/cm ratio of 0.45.

Fig. 15 presents the DSC trace for the surface part of the sample obtained from the OPC paste stored in 5% sodium sulfate solution; it displays three endothermic peaks at 115, 157 and 484 °C, indicating thaumasite, gypsum and portlandite, respectively. In the SFl0 paste immersed in 5% sodium sulfate solution, shown in Fig.

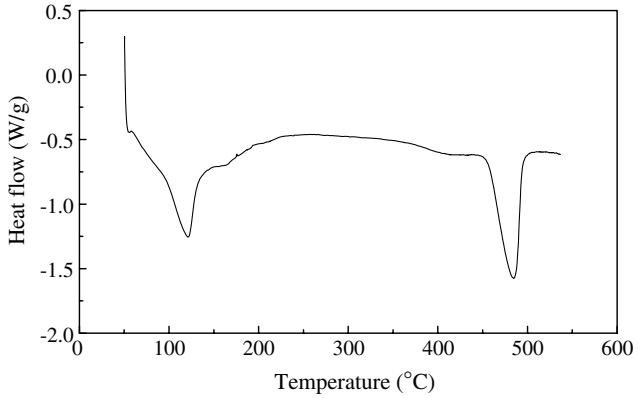

Fig. 15. DSC curve of OPC paste subjected to sulfate attack in 5% sodium sulfate solution for 270 days.

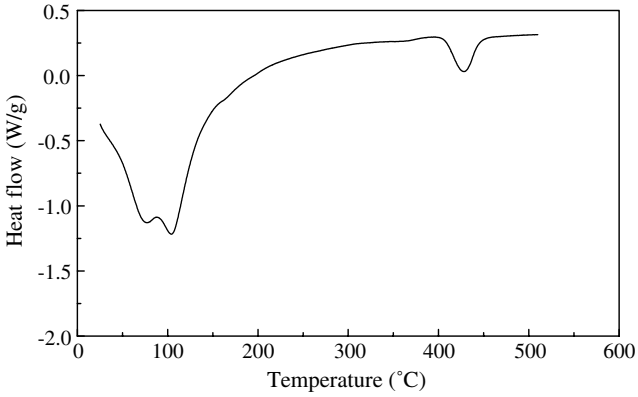

Fig. 16. DSC curve of SF10 paste subjected to sulfate attack in 5% sodium sulfate solution for 270 days.

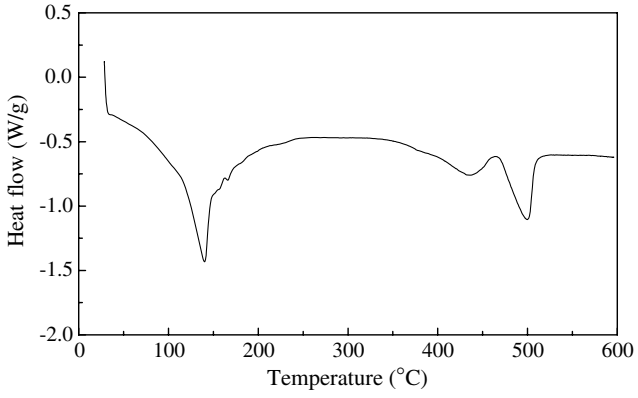

Fig. 17. DSC curve of OPC paste subjected to sulfate attack in 5% magnesium sulfate solution for 270 days.

16, the endothermic peak for portlandite at 428 °C was smaller and indicates an enthalpy of 37.04 J/g, while the endothermic peak for portlandite in the paste (Fig. 15) showed an enthalpy of 136.5 J/g. The pozzolanic reaction and the microfiller effect of silica fume are considered to have contributed to this reduction in this enthalpy value of the portlandite endothermic peak.

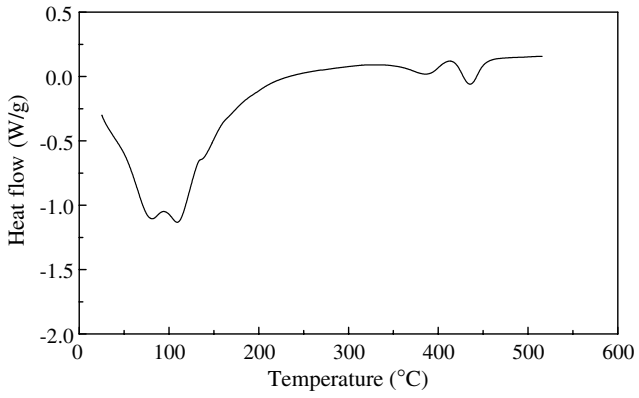

Fig. 18. DSC curve of SF10 paste subjected to sulfate attack in 5% magnesium sulfate solution for 270 days.

In the case of the paste samples immersed in 5% magnesium sulfate solution, the endothermic peak for brucite produced by the reaction with Mg^{2+} ions and $Ca(OH)_2$ is conspicuously present in their DSC curves, as shown in Figs. 17 and 18. As expected, the enthalpy of the SF10 paste powder (20.40 J/g) was significantly smaller than that of the OPC paste powder (53.30 J/g) in proportion to the enthalpy for the brucite endothermic peak. The enthalpy for the portlandite in the DSC curves of OPC and SF10 pastes is similar to that in sodium sulfate solution.

One point worth emphasizing is the occurrence of the double peak in the DSC traces in the temperature region 70–130 °C in the SF paste samples exposed to both sodium and magnesium sulfate solutions (Figs. 16 and 18) which are not present in the OPC paste samples (Figs. 15 and 17). It is thought that these double peaks could be attributed to the formation of secondary C–S–H which is less dense compared to primary C–S–H.

5. Discussion of test results

Sulfate attack on the Portland cement matrix is, generally, characterized by the reaction of sulfate ions with the cement hydration products which causes expansion, cracking and spalling, as well as loss of mass and strength [9,10,21–23]. Numerous studies to minimize the attack, and prolong the service life of concrete structures exposed to sulfate environments have been carried out. All these studies show that sulfate attack is the result of a complex set of chemical processes, and that there is still a lot of controversy about the mechanism of such attack.

From visual examination, it is clear that mortar specimens stored in a sodium sulfate solution behave very differently from those exposed to a magnesium

sulfate solution with respect to the form and degree of deterioration. In this study, detailed visual examination was carried out periodically, and the results are summarized in Table 3. For the OPC-45 mortar specimen, the most marked difference between sodium sulfate attack and magnesium sulfate attack was a visible loss of mass, as shown in Figs. 1 and 3. The significant expansion of the OPC mortar specimen, and the consequent disintegration seems to be responsible for the considerable mass loss in sodium sulfate solution. On the other hand, the mass loss of SF mortar specimens stored in sodium sulfate solution was negligible even after 510 days. The beneficial effect of SF in a 5% sodium sulfate solution is thus clearly observed in this study. Under this sulfate environment, the incorporation of 10% SF in the OPC matrix showed no evidence of spalling and cracking up to about 1 year of exposure. These results are in agreement with those reported by Wee et al. [21] which showed that silica fume, at replacement levels of 5% and 10% by mass of OPC plays a key role in resisting sodium sulfate attack, indicating no signs of spalling after about 1 year of exposure in 5% sodium sulfate solution.

Unlike the role of SF in mortar specimens exposed to 5% sodium sulfate solution, mortar specimens with SF displayed more severe deterioration, compared with OPC mortar specimens, after 180 days of exposure to magnesium sulfate solution. With the OPC mortar there is abundant calcium hydroxide at the surface to react with magnesium sulfate to form brucite and gypsum. However, partial replacement of OPC with SF reduces calcium hydroxide availability due to the pozzolanic reaction and allows the magnesium sulfate to more easily attack the C–S–H, leading to decalcification, M–S–H formation and destruction of the cement bond. In addition, gypsum rather than ettringite would tend to form because of locally reduced pH and the limited local availability of aluminium [8,22], as confirmed by the XRD data.

Although OPC mortar specimens produced more brucite on the surface, they were less deteriorated than SF mortar specimens. This implies that the deterioration of the SF mortar due to magnesium sulfate attack is mainly dependent on the formation of M–S–H (or Mg-rich C–S–H gel) rather than the surface double layer, consisting of brucite and gypsum. However, further attack and disintegration could be expected once the double-layer has significantly peeled off.

The compressive strength loss (CSL) of mortar specimens presented in Figs. 5–10 corresponded well with the visual examination reported in Table 3. In particular, the almost linear increase of CSL with immersion age of OPC mortar specimens placed in 5% sodium sulfate solution shown in Fig. 5 is an indication of the predominant effect of severe softening and expansion in these mortar specimens. The SF mortar specimens in the same solution, on the other hand, showed no significant increase in CSL after 270 days of exposure. As stated earlier, the relatively large amount of calcium hydroxide and C_3A in the OPC system led to the drastic increase in the CSL of mortar specimens, because of the increased formation of ettringite and gypsum. However, the reverse trend appeared when mortar specimen with or without SF is attacked by magnesium sulfate solution (Fig. 10). Similar studies reported in literature [9,15], confirm a considerable strength reduction of cement systems with silica fume under magnesium sulfate attack. The sharp increase in CSL of OPC-45 mortar specimens after 360 days of exposure may have resulted from the disruption of the surface double-layer in the system. As shown in Figs. 5 and 8, the overall CSL of OPC mortars in magnesium sulfate solution was much less pronounced than that in sodium sulfate solution. The CSL in the two solutions corresponded very well with the observed expansion, cracking and mass loss of OPC test samples in the respective solution. This trend was confirmed by continued exposure in sodium sulfate solution for 510 days, where the cracking extended throughout the test specimens leading to extensive spalling and mass loss. Other studies [9,22] have reported higher CSL of OPC mortar in magnesium sulfate solution than in sodium sulfate solution although the samples showed much greater expansion in the sodium sulfate environment. Several factors are probably involved in this apparent discrepancy, but a discussion of these is beyond the scope of this paper.

Mineralogical analyses based on XRD clearly support the results of CSL of mortar specimens. Especially after about 180 days of exposure, the XRD trace for the surface part of OPC-45 mortar specimens subjected to sodium sulfate attack confirmed the formation of ettringite by its peak at 9.1° 2θ, although the intensity of the peak was somewhat weak. Continued exposure (360 and 510 days) led to the formation of a large amount of gypsum crystals, as could be observed in the XRD analysis (Fig. 11). The formation of gypsum when exposed to sodium sulfate solution seems to have been associated with considerable expansion and strength loss in the mortar system. On the contrary, there was only slight evidence of the formation of gypsum in the surface of SF10-45 mortar specimens even though they were subjected to attack for 510 days (Fig. 12). This explains why the CSL values of these specimens were relatively smaller than those of the OPC mortar specimens.

In the magnesium sulfate environment, further attack of SF mortar specimens, which is related to the compressive strength loss, was observed. In the presence of SF, it is suggested that adjacent to the surface double-layer, ingress of magnesium ions and subsequent reaction with the disintegrated C–S–H gel gave Mg-rich C–S–H or M–S–H. These products would mainly

prevail in the SF mortar system subjected to magnesium sulfate attack, and could not generally be detected by XRD because of their poor crystallinity [24]. In other words, it is concluded that SF helps to resist the sodium sulfate attack, but aggravates the magnesium attack [9].

The observations identified from XRD traces are also largely confirmed by DSC analysis on paste samples, although the latter microstructural observations were carried out at a different immersion age. The solid phases detected in XRD patterns for mortar specimens exposed to sulfate test solutions are summarized in Table 5. The following peaks were used as indicators for solid phases in XRD patterns: ettringite (9.1), thaumasite (9.2°), gypsum (11.7°), portlandite (18.1°) and brucite (38.0°). The products identified by XRD in this study, seem not to be consistent with DSC results. This inconsistency in the results of DSC and XRD analysis may be attributed to the differences in the deterioration stages of mortars (510 days) and pastes (270 days).

Additionally, Figs. 19 and 20 show the SEM image of the surface part of OPC mortar stored in 5% magnesium sulfate solution for 510 days and the EDS spectra of points A–C, respectively. It is evident that the reaction with sulfate or magnesium ions, and calcium hydroxide produces the double layer consisting of brucite and gypsum, as shown in the EDS spectrum at point A in Fig. 20. Strong peaks for Mg and O are observed at the point B, indicating that this is brucite, according to the following equation.

$$MgSO_4 + Ca(OH)_2 + 2H_2O \rightarrow Mg(OH)_2 + CaSO_4 \cdot 2H_2O$$

The EDS spectrum at point C is consistent with gypsum formation. These phenomena agree well with the study reported by Bonen and Cohen [25].

6. Concluding remarks

This paper presents a detailed study on the process of deterioration and the formation of reactants by chemical reaction of mortars and pastes without or with SF in sodium and magnesium sulfate solutions.

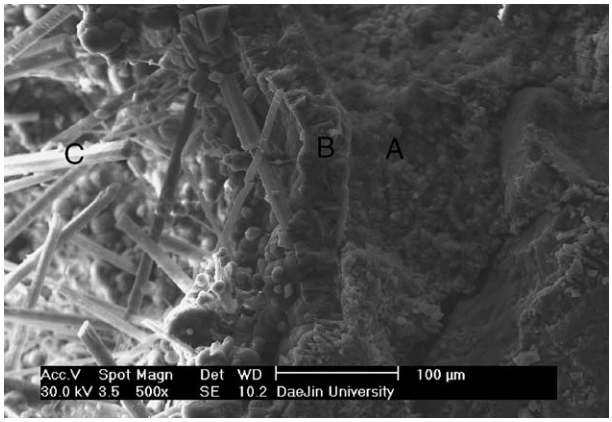

Fig. 19. SEM image of OPC paste exposed to a 5% magnesium sulfate solution for 510 days.

In the sodium sulfate environment, the use of SF has a beneficial effect in terms of controlling the strength loss of OPC mortar specimens due to its strong pozzolanic reaction and the consequent reduction of calcium hydroxide. The SF mortars do not easily permit the permeation and diffusion of sulfate ions originating from the sodium sulfate solution. The capability for higher absorption of sulfate ions into OPC mortar specimens compared to that into SF mortar specimens may explain the severe deterioration of the former, especially in terms of compressive strength loss. Expansion, spalling and considerable mass loss are also characterized as the degradation process of OPC mortars by sodium sulfate attack progresses. After 510 days of immersion in 5% sodium sulfate solution, OPC mortar with a w/cm ratio of 0.55 exhibited a CSL value as high as 92%, while SF10-55 mortar displayed a strength loss of only about 42%. Visual examination confirmed the excellent sulfate resistance of SF mortars irrespective of the w/cm ratio and the level of cement replacement.

In the magnesium sulfate environment, the continuing formation of secondary gypsum layers was ob-

Table 5
Summary of solid phases detected by XRD trace on the surface of mortar specimens exposed to sulfate test solutions

Immersion age (days)	Symbol	5% sodium sulfate solution				5% magnesium sulfate solution				
		E	T	G	P	E	T	G	P	B
91	OPC-45	O			O	O		O	O	
	SF10-45				O	O			O	
180	OPC-45	O		O	O	O		O	O	O
	SF10-45				O	O	O	O		
360	OPC-45	O	O	O	O	O	O	O		O
	SF10-45	O					O	O		O
510	OPC-45	O	O	O		O	O	O		O
	SF10-45	O					O	O		O

Note: E = ettringite, T = thaumasite, G = gypsum, P = portlandite, B = brucite.

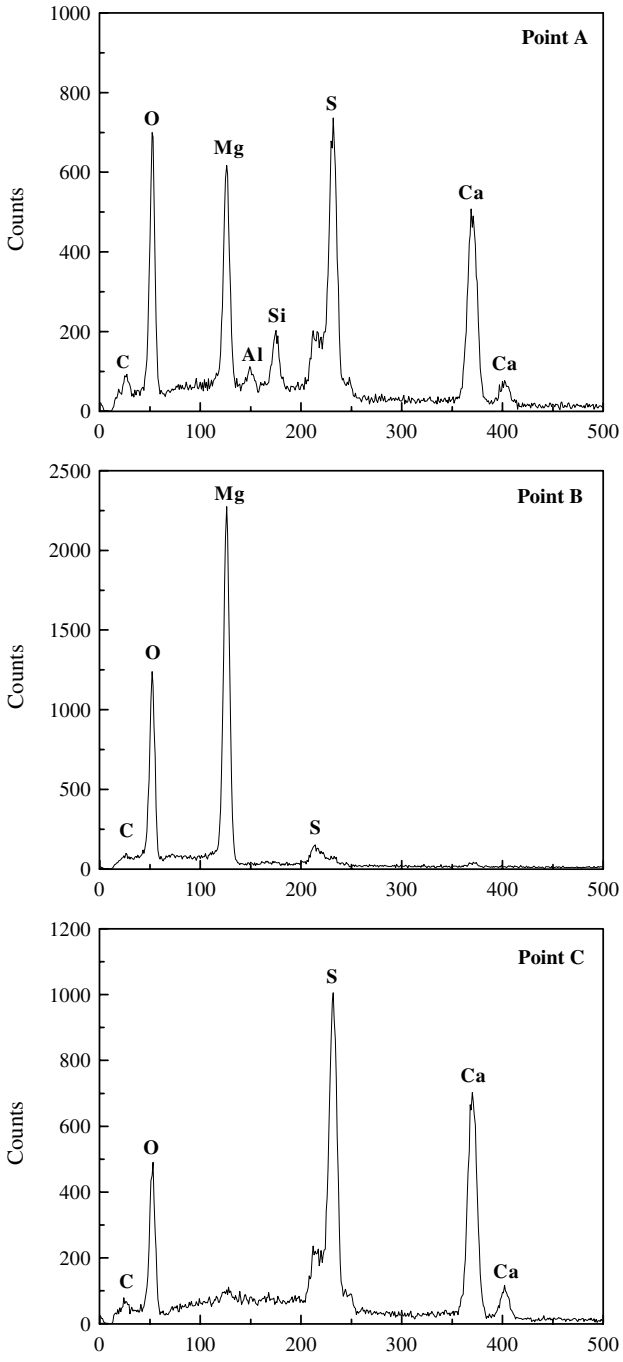

Fig. 20. EDS spectra obtained from pointed area in Fig. 19.

served in the OPC mortar. This observation results from the dissociation of calcium hydroxide and decalcification of C–S–H. The CSL data of mortars due to magnesium sulfate attack emphasized that the presence of SF showed a negative effect, resulting in additional loss of mass and reduction in specimen cross-section, compared with those of OPC mortars. With respect to w/cm ratio, the trends on CSL of mortar specimens with and without SF attacked by magnesium sulfate solution were similar to those in sodium sulfate solution. On the other hand, in magnesium sulfate environment, the larger the amount of SF content, the greater was the strength loss exhibited.

There was excellent correspondence between strength loss and the visually observed cracking, spalling and mass loss of OPC mortars in the two sulfate solutions. This agreement was further confirmed by the continued exposed of the OPC test specimens in sodium sulfate solutions for 810 days.

Although the enthalpy for brucite in the SF cement system, as shown by DSC curves, was smaller than that in the OPC system, SF mortars had a lower resistance to magnesium sulfate attack, in terms of CSL, compared with that of OPC mortar. This phenomenon may be largely due to the possible conversion of C–S–H into M–S–H, which is non-cementitious.

The presence of gypsum and thaumasite in the surface layer of mortar with or without SF in magnesium sulfate environment was also confirmed through XRD analysis. The double layer, consisting of brucite and gypsum, in the surface zone of the cement system seems to have peeled off due to loss of cohesion between the sound inner core and the more disintegrated outer part deteriorated by sulfate attack.

References

[1] Harboe EM. Longtime studies and field experiences with sulfate attack. In: Sulfate resistance of concrete (George Verbeck Symposium), ACI SP-77, 1982, p. 1–20.
[2] Figg A. Field studies of sulfate attack on concrete. In: Marchand J, Skalny J, editors. Material science of concrete special volume: sulfate attack mechanisms. Westerville, OH: The American Ceramic Society; 1999. p. 315–24.
[3] Collepardi M. Thaumasite formation and deterioration in historic buildings. Cem Concr Compos 1999;21:147–54.
[4] Brown PW, Doerr A. Chemical changes in concrete due to the ingress of aggressive species. Cem Concr Res 2000;30:411–8.
[5] Hobbs DW, Taylor MG. Nature of the thaumasite sulfate attack mechanism in field concrete. Cem Concr Res 2000;30:529–33.
[6] Lawrence CD. The influence of binder type on sulfate resistance. Cem Concr Res 1992;22:1047–58.
[7] Al-Amoudi OSB, Rasheeduzzafar, Maslehuddin M, Abduljauwad SN. Influence of chloride ions on sulphate deterioration of plain and blended cements. Mag Concr Res 1994;46(167):113–23.
[8] Rasheeduzzafar, Al-Amoudi OSB, Abduljauwad SN, Maslehuddin M. Magnesium-sodium sulfate attack in plain and blended cements. ASCE J Mater Civil Eng 1994;6(2):201–22.
[9] Al-Amoudi OSB, Maslehuddin M, Saadi MM. Effect of magnesium sulfate and sodium sulfate on the durability performance of plain and blended cements. ACI Mater J 1995;92(1):15–24.
[10] Torii K, Taniguchi K, Kawamura M. Sulfate resistance of high fly ash content concrete. Cem Concr Res 1995;25:759–68.
[11] Akoz F, Turker F, Koral S, Yuzer N. Effects of sodium sulfate concentration on the sulfate resistance of mortars with and without silica fume. Cem Concr Res 1995;25:1360–8.
[12] Khatri RP, Sirivivatnanon V. Role of permeability in sulphate attack. Cem Concr Res 1997;27:1179–89.
[13] Moon HY, Lee ST, Kim HS. The selection of effective Korean cement for sulfate environments. In: Proceeding of the 3rd

International Conference on Concrete Under Severe Conditions, Canada, 2001. p. 349–56.
[14] Taylor HFW. Cement chemistry. 2nd ed. London: Thomas Telford; 1997.
[15] Cohen MD, Bentur A. Durability of Portland cement–silica fume pastes in magnesium sulfate and sodium sulfate solutions. ACI Mater J 1988;85(3):148–57.
[16] Cohen MD, Mather B. Sulfate attack on concrete—research needs. ACI Mater J 1991;88(1):62–9.
[17] Gollop RS, Taylor HFW. Microstructural and microanalytical studies of sulfate attack. Cem Concr Res 1992;22:1027–38.
[18] Bonen DA. Microstructural study of the effect produced by magnesium sulfate on plain and silica fume-bearing Portland cement mortars. Cem Concr Res 1993;23:541–53.
[19] Turker F, Akoz F, Koral S, Yuzer N. Effects of magnesium sulfate concentration on the sulfate resistance of mortars with and without silica fume. Cem Concr Res 1997;27:205–14.
[20] Mangat PS, El-Khatib JM. Influence of initial curing on sulphate resistance of blended cement concrete. Cem Concr Res 1992; 22:1089–100.
[21] Wee TH, Suryavanshi AK, Wong SF, Anisur Rahman KM. Sulfate resistance of concrete containing mineral admixture. ACI Mater J 2000;97(5):536–49.
[22] Al-Amoudi OSB. Sulfate attack and reinforcement corrosion in plain and blended cements exposed to sulfate environments. Build Environ 1998;33(1):53–61.
[23] Al-Amoudi OSB. Attack on plain and blended cements exposed to aggressive sulfate environments. Cem Concr Compos 2002; 24:305–16.
[24] Skalny J, Marchand J, Odler I. Sulfate attack on concrete. 1st ed. London: Spon Press; 2002.
[25] Bonen D, Cohen MD. Magnesium sulfate attack on Portland cement paste—II. Chemical and mineralogical analyses. Cem Concr Res 1992;22:707–18.